



## King's Research Portal

*Document Version*  
Peer reviewed version

[Link to publication record in King's Research Portal](#)

*Citation for published version (APA):*

Prickett, A., Montibus, B., Barkas, N., Amante, S., Franco, M., Cowley, M., Puszyk, W., Shannon, M., Irving, M., Madon-Simon, M., Ward, A., Schulz, R., Baldwin, H. S., & Oakey, R. (2021). Imprinted gene expression and function of the dopa decarboxylase gene in the developing heart. *Frontiers in Cell and Developmental Biology*, 00(00), 00. Article 00. Advance online publication.

### **Citing this paper**

Please note that where the full-text provided on King's Research Portal is the Author Accepted Manuscript or Post-Print version this may differ from the final Published version. If citing, it is advised that you check and use the publisher's definitive version for pagination, volume/issue, and date of publication details. And where the final published version is provided on the Research Portal, if citing you are again advised to check the publisher's website for any subsequent corrections.

### **General rights**

Copyright and moral rights for the publications made accessible in the Research Portal are retained by the authors and/or other copyright owners and it is a condition of accessing publications that users recognize and abide by the legal requirements associated with these rights.

- Users may download and print one copy of any publication from the Research Portal for the purpose of private study or research.
- You may not further distribute the material or use it for any profit-making activity or commercial gain
- You may freely distribute the URL identifying the publication in the Research Portal

### **Take down policy**

If you believe that this document breaches copyright please contact [librarypure@kcl.ac.uk](mailto:librarypure@kcl.ac.uk) providing details, and we will remove access to the work immediately and investigate your claim.

# Imprinted gene expression and function of the dopa decarboxylase gene in the developing heart

Adam R. Prickett<sup>1</sup>, Bertille Montibus<sup>1</sup>, Nikolaos Barkas<sup>1</sup>, Samuele M. Amante<sup>1</sup>, Maurício M. Franco<sup>1</sup>, Michael Cowley<sup>1</sup>, William Puszyk<sup>1</sup>, Matthew F. Shannon<sup>1</sup>, Melita Irving<sup>2</sup>, Marta Madon-Simon<sup>3</sup>, Andrew Ward<sup>3</sup>, Reiner Schulz<sup>1</sup>, H S. Scott Baldwin<sup>4</sup>, Rebecca J. Oakey<sup>1\*</sup>

<sup>1</sup>King's College London, United Kingdom, <sup>2</sup>Guy's and St Thomas' NHS Foundation Trust, United Kingdom, <sup>3</sup>University of Bath, United Kingdom, <sup>4</sup>Vanderbilt University, United States

*Submitted to Journal:*  
Frontiers in Cell and Developmental Biology

*Specialty Section:*  
Developmental Epigenetics

*Article type:*  
Original Research Article

*Manuscript ID:*  
676543

*Received on:*  
05 Mar 2021

*Revised on:*  
17 May 2021

*Journal website link:*  
[www.frontiersin.org](http://www.frontiersin.org)

### *Conflict of interest statement*

The authors declare that the research was conducted in the absence of any commercial or financial relationships that could be construed as a potential conflict of interest

### *Author contribution statement*

AP conducted experiments, interpreted data and contributed to writing the paper, SMA, MF, MC, WP, MS conducted experiments; MDI collected human tissue samples; BM, NB, RS designed and performed data analyses; MM-S and AW provided and collected Grb10 transgenic tissue samples; HSB conceived the EFIC analysis and provided EFIC facilities, supervised AP and interpreted the heart sections and EFIC data; RJO conceived the project, supervised the project, interpreted the data and wrote the paper with AP. All authors contributed to the critical reading of the manuscript.

### *Keywords*

Dopadecarboxylase, knock-out, imprinting, Heart, Mouse, human

### *Abstract*

Word count: 196

Dopa decarboxylase (DDC) synthesises serotonin in the developing mouse heart where it is encoded by *Ddc\_exon1a*, a tissue-specific paternally expressed imprinted gene. *Ddc\_exon1a* shares an imprinting control region (ICR) with the imprinted, maternally expressed (outside of the central nervous system) *Grb10* gene on mouse chromosome 11, but little else is known about the tissue-specific imprinted expression of *Ddc\_exon1a*. Fluorescent immunostaining localises DDC to the developing myocardium in the pre-natal mouse heart, in a region susceptible to abnormal development and implicated in congenital heart defects in human. *Ddc\_exon1a* and *Grb10* are not co-expressed in heart nor in brain where *Grb10* is also paternally expressed, despite sharing an ICR, indicating they are mechanistically linked by their shared ICR but not by *Grb10* gene expression. Evidence from a *Ddc\_exon1a* gene knockout mouse model suggests that it mediates the growth of the developing myocardium and a thinning of the myocardium is observed in a small number of mutant mice examined, with changes in gene expression detected by microarray analysis. Comparative studies in the human developing heart reveal a paternal expression bias with polymorphic imprinting patterns between individual human hearts at *DDC\_EXON1a*, a finding consistent with other imprinted genes in human.

### *Contribution to the field*

Genomic imprinting confers parent-of-origin-specific gene expression on a small group of genes, largely associated with growth and development in the mammalian embryo. The study of imprinted gene expression mechanisms has revealed much about how epigenetic factors work in developmental contexts and has generated robust models applicable to non-imprinted gene expression. The Dopa decarboxylase gene (*Ddc*) encodes a highly tissue-specific isoform *Ddc\_exon1a*, whose expression is limited to the paternal allele in the developing heart. Congenital heart defects represent the leading non-infectious cause of death in the first four years of life globally and are the most common form of congenital malformations occurring in ~1% of live births. Therefore, delineating the spatial distribution of gene expression and unravelling mechanisms underpinning tissue-specific gene regulation is important for understanding heart development. Drawing on gene knock-out strategies in the mouse, the phenotype resulting from *Ddc\_exon1a* loss is examined using high-resolution 3D imaging and genome wide expression assays. Comparative imprinting studies in human fetal hearts suggest that this gene is similarly imprinted across species albeit in a less stringent way.

### *Funding statement*

This work was supported by the British Heart Foundation Project Grant [PG/13/35/30236] (RJO) and PhD studentship FS/08/051/25748 (undertaken by ARP); the Wellcome Trust [084358/Z/07/Z] (RJO); the Medical Research Council Project Grant [G1001689] (RJO); the National Institutes of Health [1R01 HL118386] (HSB); and EFIC facility, the National Institute of Health [S10-RR27661] (HSB).

## *Ethics statements*

### *Studies involving animal subjects*

Generated Statement: The animal study was reviewed and approved by Ddc knockout model generation (DdcGt(OST129277)Lex (B6;129S5-DdcGt(neo)420Lex, ID# 11693-UCD) was carried out by Lexicon Genetics Inc, USA and breeding, genotyping and tissue acquisition by the UC Davis mouse biology program. Only frozen tissues were shipped out to the laboratory.

Work involving Grb10 animals was approved by the University of Bath Animal Welfare and Ethical Review Body and carried out under UK Home Office licence (PPL 30/2839).

### *Studies involving human subjects*

Generated Statement: The studies involving human participants were reviewed and approved by Joint Research Ethics Committee of London, Camberwell St Giles, project ID 53717. The patients/participants provided their written informed consent to participate in this study.

### *Inclusion of identifiable human data*

Generated Statement: No potentially identifiable human images or data is presented in this study.

In review

### *Data availability statement*

Generated Statement: The datasets presented in this study can be found in online repositories. The names of the repository/repositories and accession number(s) can be found in the article/supplementary material.

In review

1 Imprinted gene expression and function of the dopa decarboxylase gene in the  
2 developing heart

3  
4 Adam R Prickett<sup>1</sup>, Bertille Montibus<sup>1</sup>, Nikolaos Barkas<sup>1a</sup>, Samuele M Amante<sup>1b</sup>,  
5 Maurício M Franco<sup>1c</sup>, Michael Cowley<sup>1d</sup>, William Puszyk<sup>1</sup>, Matthew F Shannon<sup>1</sup>,  
6 Melita D Irving<sup>1,3</sup>, Marta Madon-Simon<sup>2</sup>, Andrew Ward<sup>2</sup>, Reiner Schulz<sup>1</sup>, H. Scott  
7 Baldwin<sup>4</sup> & Rebecca J Oakey<sup>1\*</sup>

8  
9 <sup>1</sup>Department of Medical & Molecular Genetics, King's College London, London, UK

10 <sup>2</sup>Department of Biology & Biochemistry & Centre for Regenerative Medicine,  
11 University of Bath, Claverton Down, Bath, UK

12 <sup>3</sup>Department of Clinical Genetics, Guy's and St Thomas' NHS Foundation Trust

13 <sup>4</sup>Department of Pediatrics (Cardiology), Vanderbilt University Medical Center,  
14 Nashville, USA

15 \* To whom correspondence should be addressed: email: rebecca.oakey@kcl.ac.uk

16  
17 Current addresses: <sup>a</sup>Human Cell Atlas Data Coordination Platform, Data Sciences  
18 Platform, Broad Institute, Cambridge, MA, USA; <sup>b</sup>Centre for Genomics and Child  
19 Health, Blizard Institute, Barts and The London School of Medicine and Dentistry,  
20 Queen Mary University of London, UK, <sup>c</sup>Embrapa Genetic Resources & Biotechnology,  
21 Laboratory of Animal Reproduction, Brasília, Federal District, Brazil; <sup>d</sup>Center for  
22 Human Health and the Environment, and Department of Biological Sciences, North  
23 Carolina State University, Raleigh, NC, USA.

25

26 **Abstract**

27 Dopa decarboxylase (DDC) synthesises serotonin in the developing mouse heart  
28 where it is encoded by *Ddc\_exon1a*, a tissue-specific paternally expressed imprinted  
29 gene. *Ddc\_exon1a* shares an imprinting control region (ICR) with the imprinted,  
30 maternally expressed (outside of the central nervous system) *Grb10* gene on mouse  
31 chromosome 11, but little else is known about the tissue-specific imprinted  
32 expression of *Ddc\_exon1a*. Fluorescent immunostaining localises DDC to the  
33 developing myocardium in the pre-natal mouse heart, in a region susceptible to  
34 abnormal development and implicated in congenital heart defects in human. *Ddc*-  
35 *\_exon1a* and *Grb10* are not co-expressed in heart nor in brain where *Grb10* is also  
36 paternally expressed, despite sharing an ICR, indicating they are mechanistically  
37 linked by their shared ICR but not by *Grb10* gene expression. Evidence from a *Ddc*-  
38 *\_exon1a* gene knockout mouse model [suggests](#) that it mediates the growth of the  
39 developing myocardium [and a thinning of the myocardium is observed in a small](#)  
40 [number of mutant mice examined, with changes in gene expression detected by](#)  
41 [microarray analysis](#). Comparative studies in the human developing heart reveal a  
42 paternal expression bias with polymorphic imprinting patterns between individual  
43 human hearts at *DDC\_EXON1a*, a finding consistent with other imprinted genes in  
44 human.

45

46 **Key Words:** Dopa-decarboxylase knock-out, imprinting, heart, human, mouse.

47 **Word count** 4445

48

49

50 **Introduction**

51 There are over a hundred imprinted genes in the mouse and human genome (Kelsey  
52 and Bartolomei, 2012) many of which contribute to mammalian growth and  
53 development (Cleaton et al., 2014). Genomic imprinting is the parent-of-origin-  
54 dependent, allele-specific expression of a gene (Ideraabdullah et al., 2008). Imprinted  
55 genes are regulated by epigenetic mechanisms including parent-of-origin-dependent,  
56 allele-specific DNA methylation of CpG-rich differentially methylated regions (DMRs).  
57 There are two classes of DMRs: germline DMRs that are established during  
58 gametogenesis are maintained throughout development and act as imprinting  
59 control regions (ICRs); and somatic DMRs that arise post-fertilization, are often  
60 tissue-specific and can contribute to the regulation of imprinted gene clusters  
61 together with the ICR (Edwards and Ferguson-Smith, 2007). Both classes are  
62 maintained during cell division (Lewis and Reik, 2006).

63

64 The Dopa decarboxylase gene (*Ddc*) has two transcript isoforms, one is expressed  
65 from both parental alleles and the other is imprinted. *Ddc*, is expressed from both  
66 parental alleles in the urinary system, eye, nervous system, liver, limbs, alimentary  
67 system and ear. Deficiency of this canonical form of the gene in humans results in an  
68 autosomal recessive inborn error of metabolism (MIM #608643) (Smith et al., 2014)  
69 (Lee et al., 2013). The second transcript isoform, known as *Ddc\_exon1a* was  
70 identified through the analysis of a differential gene expression screen designed to  
71 detect novel imprinted genes and it is imprinted, being expressed only from the  
72 paternally inherited allele in the developing mouse heart (Menheniott et al., 2008).



73

74 Imprinted genes are typically found in clusters in the genome (Barlow and Bartolomei,  
75 2014) and *Ddc\_exon1a* is no exception lying adjacent to *Grb10*, an imprinted gene  
76 that encodes an intracellular signalling adaptor protein. *Grb10* is typically maternally  
77 expressed (Charalambous et al., 2003) and acts to restrict fetal growth and promote  
78 adipose deposition in adulthood (Smith et al., 2007; Madon-Simon et al., 2014).  
79 Unusually, *Grb10* is expressed from the opposite (paternal) allele in the CNS but the  
80 mechanism that underlies this switch between maternal and paternal expression is  
81 unclear, as is the role for paternally expressed *Grb10* in neurons (Plasschaert and  
82 Bartolomei, 2015). The two genes therefore comprise an imprinting cluster where  
83 imprinted expression is directed via the shared ICR in the 5' untranslated region (UTR)  
84 of *Grb10* (also known as the *Grb10* CpG island 2 (CGI 2) DMR). When the ICR is ablated,  
85 it results in loss of both *Grb10* and *Ddc\_exon1a* imprinting (Shiura et al., 2009). Since  
86 the regulation of imprinted gene clusters is typically co-ordinated (Ideraabdullah et  
87 al., 2008), we reasoned that *Ddc\_exon1a* expression could be co-ordinately regulated  
88 with the expression of *Grb10*.

89

90 *Ddc\_exon1a* is the only variant of *Ddc* expressed in heart and is a unique example of  
91 a transcript that shows heart-specific genomic imprinting. *Grb10* has a more complex  
92 imprinted expression pattern in the developing embryo but exhibits paternal  
93 expression in the CNS. There are varying reports regarding *Ddc\_exon1a* expression in  
94 the brain (Shiura et al., 2009; Madon-Simon et al., 2014; Smith et al., 2014;  
95 Plasschaert and Bartolomei, 2015). As *Grb10* is expressed maternally in most tissues  
96 but shows paternal expression specifically in the brain and in subsets of cells in the

97 heart, this suggested to us that *Ddc\_exon1A* and *Grb10* might be linked and  
98 coordinately expressed in brain and heart.

99  
100 We sought to investigate the allelic expression of *Ddc\_exon1a* in the brain and the  
101 heart using allele-specific assays in tissues from reciprocal hybrid mouse strains. As  
102 allelic expression was predominantly observed in the heart, the spatial pattern of  
103 DDC\_EXON1A protein was delineated in the developing mouse heart by  
104 immunostaining embryonic sections. Spatial distribution was also compared to its ICR  
105 partner *Grb10* in a gene trap transgenic mouse line. To investigate function, the  
106 phenotype of a knockout mouse model of *Ddc\_exon1a* was examined and changes in  
107 the developing myocardium were seen along with gene expression changes  
108 associated with tissue development and cellular organisation. An antisense transcript  
109 overlaps *Ddc\_exon1a* but no evidence was found for it influencing imprinted  
110 *Ddc\_exon1a* expression *in cis*. A comparative study examining the expression of  
111 DDC\_EXON1A in 40 human fetal hearts including fetal-maternal pairs, reveals a  
112 paternal expression bias and a polymorphic pattern of imprinted gene expression.

113

## 114 **Materials and Methods**

### 115 **Allele-specific RT-PCR assays**

116 RNA was extracted from tissue using the RNAeasy Kit<sup>TM</sup> (Qiagen), assessed for purity  
117 using nanodrop (requiring a 260/280 ratio of ~2.0) and integrity using Agilent 2100  
118 Bioanalyzer, and converted to cDNA with a Superscript II<sup>TM</sup> (Invitrogen) kit, as per  
119 manufacturers' instructions. For mouse *Ddc\_exon1a* the allele was identified via a  
120 G/A single nucleotide polymorphism (SNP) between *Mus musculus domesticus*

121 C57BL/6J (B) and *Mus musculus castaneus* CAST/EiJ (C) in exon 3 (mm9,  
122 chr11:11776278). Transcripts with this SNP were amplified by PCR from reciprocal  
123 BxC and CxB hybrids (by convention, the maternal genotype is listed first) and  
124 sequenced. *Ddc\_exon1a* and *Ddc\_canonical* transcripts were amplified using exon-  
125 specific forward primers EXON1A-F (5'-TGTCACCAAGGAGAGAGAGAGA-3') and  
126 EXON1-F (5'- AGTTGTGTGCCACCTCCT-3') and a common reverse primer, EXON4-R  
127 (5'-CAGCTCTTCCAGCCAAAAG-3'). PCR: 94°C for 3 min, 34 cycles of 94°C for 30s,  
128 56°C for 30s, and 72°C for 1 min, with a final extension of 72°C for 5 min and Sanger  
129 sequencing using an ABI 3730xl.

130 For AK0066690, nested primers were used AK006690\_F\_outer:  
131 CCAGCCTCCATTCAGAGTT, AK006690\_R\_outer: TTGACTAGGAATATTCCTTCAT,  
132 amplicon size: 250bp. Inner primers were AK006690\_F\_inner:  
133 TTCAGCCAAGAGTGCTTAGG, AK006690\_R\_inner: GCTGCTGCATGCTTATTTGT,  
134 amplicon size: 184bp.

### 135 **Immunostaining**

136 e15.5 wildtype embryos were fixed in 4%PFA for 1 hour at 4°C, dehydrated and  
137 embedded in paraffin wax. Antigen retrieval was performed by boiling in high pH  
138 antigen unmasking solution (Vector Labs). Slides were blocked with 4% v/v donkey  
139 serum (abcam, ab7475) for 1.5 hours. Primary antibodies in the following dilutions:  
140 anti-DOPA Decarboxylase antibody (ab3905) (1:500), goat- $\alpha$ -mouse ANF (1:100) in  
141 0.01% Tween-20, 2% v/v donkey serum in PBS were dropped onto slides and  
142 incubated in a humidified chamber at 4°C for 16 hours. Slides were washed 3X in  
143 0.01% Tween-20 in PBS. Secondary antibodies Alexa Fluor 555 donkey- $\alpha$ -goat  
144 (Invitrogen) and Alexa Fluor 647 donkey- $\alpha$ -rabbit (Invitrogen) were diluted 1:300 in

145 0.01% Tween-20 PBS, dropped onto slides and incubated for 2 hours at RT in the dark.  
146 Slides were washed 3X in PBS and mounted using ProLong® Gold Antifade Reagent  
147 with DAPI (Invitrogen)

#### 148 **Histological analysis**

149 Histological analysis was performed on the *Grb10KO* with a *lacZ* reporter construct at  
150 the 3' end of exon 8 (Garfield et al., 2011). Gestating *Grb10KO* females were sacrificed  
151 at 18.5 days *post coitum* and the uterine horns isolated immediately. All animal  
152 experiments were approved and regulated by the university ethics committee at the  
153 University of Bath and conform to the guidelines from Directive 2010/63/EU of the  
154 European Parliament on the protection of animals used for scientific purposes. The  
155 reporter insertion ablates all isoforms of *Grb10* in mouse embryos and results in a  
156 null. Where *Grb10* expression is perturbed, *lacZ* protein expression occurs. In  
157 *Grb10<sup>+/-KO</sup>* mice, tissue localization of *Grb10* is blue with X-gal staining. *Grb10<sup>+/-KO</sup>* e15.5  
158 embryos were fixed in 4% (w/v) PFA, cryoprotected in 30% sucrose and embedded in  
159 OCT. Sections were stained for paternal *Grb10* in 1 mg/ml X-gal diluted in stain base  
160 (30mM  $K_4Fe(CN)_6$  30mM  $K_3Fe(CN)_6 \cdot 3H_2O$ , 2mM  $MgCl_2$ , 0.01% (w/v) sodium  
161 deoxycholate, 0.02% (v/v) Igepal CA-630 in 0.1% PBS) for 18 hours at 28°C and  
162 counterstained using nuclear fast red.

163 Samples were stained for DDC using VECTASTAIN® ABC kit (Vector Labs) with blocking  
164 in 5% skim milk. DDC antibody (Abcam, #3905) was used at a 1:500 dilution. Sections  
165 were counterstained with Harris' haematoxylin (30 seconds), and incubation in  
166 Scott's tap water (Fisher) for 1 minute.

#### 167 **Morphological analysis using Episcopic Fluorescence Image Capture (EFIC)**

168 Embryos and dissected neonatal mouse hearts were fixed and embedded in paraffin  
169 as for immunostaining. Measurements of embryos were adjusted to the crown rump  
170 length to account for differences in embryo size due to variation in the time of  
171 conception on a given day of gestation as is convention. For EFIC analysis (Rosenthal  
172 et al., 2004) sections were re-embedded in red aniline dyed wax and photographed  
173 using an EFIC system at Vanderbilt University, with a sectioning size of 5µm. Samples  
174 were photographed at a magnification of 20x using appropriate mCherry and GFP  
175 wavelengths. Images were quality controlled by visual inspection and rebuilt in 3D  
176 using Volocity™ image analysis software (Perkin Elmer) and virtually re-sectioned in  
177 a plane that bisected the mitral and aortic valve, with the measurements taken on  
178 this plane at the base of the papillary muscle to ensure samples were measured  
179 equally. All measurements were made blind with the identity of the samples only  
180 revealed prior to statistical analysis. Comparisons between sample groups were  
181 made using an unpaired Student's T-test.

#### 182 **Microarray analysis**

183 Microarray libraries were generated as per manufacturers' instructions for Affymetrix  
184 Genechips™ on three *Ddc*<sup>WT</sup> and four maternally deleted (*Ddc*<sup>MATΔ</sup>) (making seven  
185 wild type samples) and four paternally deleted (*Ddc*<sup>PATΔ</sup>) and one homozygous  
186 mutant (*Ddc*<sup>ΔΔ</sup>) (providing five knockouts of *Ddc\_exon1a* in embryonic heart) using  
187 two separate six-lane arrays. Raw probe signals were background-corrected using  
188 NEQC quartile-normalised and a linear model was fitted to compare the effects of  
189 different genotypes in LIMMA (Smyth, 2004). These data have been deposited in  
190 GEO, Accession number GSE87595.

#### 191 **Western blotting**

192 An e15.5 embryo carcass was macerated in 1ml of RIPA buffer (50 mM Tris-HCl (pH  
193 7.5), 150mM NaCl, 1mM EDTA, 1% (w/v) sodium deoxycholate, 0.1% SDS, 1mM  
194 PMSF, 1x protease inhibitor (Roche)) and centrifuged at 16000g for 20 mins at 4°C.  
195 Total protein in the supernatant was measured using the BCA protein assay kit  
196 (Pierce) and stored at -20°C. The same protocol was used to extract protein from  
197 cultured cells without maceration. 20µg in 25µl of each sample was mixed 1:1 with  
198 2x reducing buffer (62.5mM Tris HCl pH 6.8, 2% (w/v) SDS, 6 M Urea, 2% (v/v) Igepal  
199 CA-630, 5% (v/v) β-mercaptoethanol, 0.02% (w/v) bromophenol blue, 4% glycerol  
200 and heated to 95°C for 5 mins. Samples were electrophoresed alongside a Spectra™  
201 multicolor protein ladder (Thermo) on a 12% polyacrylamide resolving gel: 12%  
202 polyacrylamide (National Diagnostics), 0.37M Tris:HCl pH 8.8, 0.1% SDS, 0.05% AMPS,  
203 0.05% TEMED with a stacking gel (5% polyacrylamide, 0.12M Tris:HCl pH 6.8, 0.05%  
204 AMPS, 0.1% TEMED) at 100V for 3 hours in running buffer (0.1% SDS, 25mM Tris,  
205 208mM glycine). Protein was transferred at 90V for 2 hours to a PVDF membrane  
206 (Bio-Rad) using western blot wet transfer buffer (25mM Tris, 192mM glycine, 20%  
207 (v/v) methanol. The membrane was blocked for 90 mins in 5% powdered skimmed  
208 milk (Marvel) in 0.1% Tween-20 with PBS. Primary antibodies were diluted, rabbit-α-  
209 mouse DDC (1:1000) in 5% milk in 0.1% Tween-20 with PBS and incubated with the  
210 membrane overnight at 4°C. Membranes were washed 3X in 0.1% Tween-20 with PBS  
211 for 15 mins and incubated in peroxidase-conjugated goat anti-rabbit secondary  
212 antibody (DAKO P0448) diluted 1:2000 in 5% milk in 0.1% Tween-20 with PBS for 1  
213 hour at RT. 3X washes were performed and protein detected using the ECL system  
214 (Amersham). Proteins were visualised by exposure to Fuji film developed on a Laser45  
215 machine. For loading control, membranes were stripped by heating at 50°C for 30

216 mins in stripping buffer (100mM 2-Mecaptoethanol, 2% SDS, 62.5mM Tris:HCl,  
217 pH6.7), washed 3X in 0.1% Tween-20 with PBS for 15 mins, and re-probed using  
218 mouse- $\alpha$ -mouse Tubulin (abcam anti-alpha Tubulin antibody ab7291; 1:5000) and  
219 rabbit- $\alpha$ -mouse Histone H3 (abcam H3 ab1791; 1:5000).

220 **Knockout mice:** *Ddc* knockout model generation was carried out by Lexicon Genetics  
221 Inc, USA and breeding, genotyping and tissue acquisition by the UC Davis mouse  
222 biology program. The mouse strain and cell lines are deposited as frozen embryos in  
223 the International Mouse Strain Resource  
224 (<http://www.informatics.jax.org/external/ko/lexicon/2095.html>) and listed in MGI as  
225  $Ddc^{Gt(OST129277)Lex}$  (B6;129S5- $Ddc^{Gt(neo)420Lex}$ , ID# 11693–UCD). Homozygous null mice  
226 have a lethal phenotype and their number is lower than Mendelian expectations at  
227 E10.5 (for example, four heterozygous inter-crosses of this knock-out mouse resulted  
228 in 11 WT, 14 Heterozygous and 3 double knock-out embryos. Mendelian ratios would  
229 have expected numbers in line with 11 WT, 22, Heterozygous and 11 double knock-  
230 out embryos) non-Mendelian ratios we also observed at litters dissected at E15.5.  
231 Heterozygous mice did not show overt phenotypes in the Lexicon Genetics high-  
232 throughput phenotype screen which aimed to identify genes that when ablated,  
233 resulted in overt phenotypes in obesity and skeletal anomalies. This screen is  
234 acknowledged to be conflicted between studying individual lines of mice and  
235 screening many lines rapidly. Therefore, compromises were made in terms of  
236 phenotypic detail, making detailed analyses of heterozygotes essential at the  
237 individual gene/strain level. Here we examine the embryos in detail for cardiac  
238 phenotypes which were not scored in the Lexicon Genetics screen. The *Grb10KO*  
239 knockout mouse strain was that described in Garfield *et al* (Garfield et al., 2011).

240 **Human tissue acquisition**

241 Twenty-five human heart and matched decidua from four to 13 weeks were provided  
242 by the MRC-Wellcome Trust Human Developmental Biology Resource (HDBR)  
243 (<http://www.hdbr.org>) from the Institute of Genetic Medicine, Newcastle and  
244 Institute of Child Health, London. Fifteen fetal heart samples and matched maternal  
245 cheek swabs were collected via an approved protocol from the Joint Research Ethics  
246 Committee of London, Camberwell St Giles, project ID 53717. Informed consent was  
247 obtained for the inclusion of these samples. The study was performed abiding by the  
248 ethical principles underlying the Declaration of Helsinki and good practice guidelines  
249 on the proper conduct of research.

250 **Human embryo allele-specific assays** by RT-PCR and Sanger sequencing. RNA was  
251 extracted from tissue and converted to cDNA using the RNAeasy™ (Qiagen) and  
252 Superscript II™ (Invitrogen) kits, as per manufacturers' instructions. gDNA was  
253 extracted using a DNAeasy kit™ (Qiagen). SNPs were identified in the UCSC genome  
254 browser and amplified with primers:

255 DDC\_13/15R:GGCATTAGCCACATGACAA–59.5

256 DDC\_13/15F:ATTCTGGGGCTTGTCTGCTT–61.2

257 DDC\_1/4F:TGGAGAATCCCATCAAGGAG–60.0

258 DDC\_1/1a/4R:CACAGTCTCCAGCTCTGTGC–59.8

259 DDC\_1a/4F:GGACAGAGAGCAAGTCACTCC–59.0

260 DDC\_1a/4F2:CTGTCACTGTGGAGAGGAGAG–57.6 and sequenced on an ABI 3730xl.

261

262 **Results**

263 ***Ddc-Exon1a* is predominantly found in the developing mouse heart**



264 Fluorescence immunostaining reveals the cellular distribution of cardiac DDC protein  
265 in e15.5 hearts. Because *Ddc-Exon1a* is the only isoform expressed in the developing  
266 heart (Menheniott et al., 2008) the staining reflects its expression. Sections in the  
267 coronal plane show a four-chamber view of the heart (Figure 1) which were either  
268 co-stained for DDC and MF-20 (an antibody to the myocardial marker myosin heavy  
269 chain) (Figure 1 A-C), or DDC and ANF (a marker of trabeculae, the complex meshwork  
270 of myocardial strands) (Figure 1 D-I). DDC protein was present throughout the  
271 ventricular myocardium and inter-ventricular septum (IVS), the structure between  
272 the right and left ventricles (Figure 1 B, E, H), but was absent from the atria and the  
273 trabecular layer, except where the trabeculae meet the compact myocardial layer  
274 (Figure 1 D-I). In addition, DDC protein was not detected in the epicardium or  
275 endocardium. Expression in cardiac fibroblasts is not ruled out, but this cell  
276 population is a small component of the ventricular wall at this stage of development  
277 (Lajiness and Conway, 2014). Scattered DDC is detected throughout the compact  
278 myocardium of both ventricles, with protein present in the myocytes of the right  
279 ventricular apex, outflow tract, and right ventricular portion of the interventricular  
280 septum at e15.5, and this same pattern was observed at e18.5 (Figure 1 E, J-L). All of  
281 these regions of the myocardium (RV apex, RV outflow tract, and RV portion of the  
282 interventricular septum) are derived primarily from progenitor cells of the secondary  
283 heart field and are particularly susceptible to abnormal development leading to  
284 congenital heart defects (Kelly, 2012).

285

286 *Ddc\_exon1a* exists in an imprinting cluster along with *Grb10* and their imprinted  
287 expression is coordinated by the *Grb10* ICR. Paternal *Grb10*, which is expressed in a

288 subset of cells in the heart, was detected using a *Grb10*-LacZ reporter transmitted  
289 through the paternal germline (Garfield et al., 2011). Its restricted expression appears  
290 punctate in the IVS and the atrio-ventricular septum (Figure 2) and is present in a  
291 small region next to the right ventricular myocardium suggestive of a coronary vessel.  
292 Paternally derived DDC\_EXON1a protein however was more broadly evident  
293 throughout the myocardium (Figure 2). DDC\_EXON1a protein and *Grb10* gene  
294 expression assays do not provide a direct comparison, but these data indicate that  
295 DDC\_EXON1a and *Grb10* are not obviously present in the same cell types by visual  
296 inspection, therefore these genes are not likely to share tissue-specific regulatory  
297 elements.

298  
299 *Ddc\_exon1a* expression was also examined in whole brain (Supplementary Figure 1),  
300 because a number of imprinted genes exhibit tissue-specific imprinting in the brain  
301 (Ferrón et al., 2011) and because of the known switch to paternal expression of *Grb10*  
302 in neuronal cells. The assay may however be limited because the glia present in whole  
303 brain tissue samples express *Grb10* reciprocally from the maternal allele, which could  
304 confound an allelic-specific assay of mixed cell types (Yamasaki-Ishizaki et al., 2007).  
305 Allele-specific assays measure the height of sequencing peaks from parental alleles  
306 and here indicate that *Ddc\_exon1a* is expressed from both parental alleles in whole  
307 brain, and in some sub-regions including the pre-optic area of the hypothalamus, the  
308 cerebellum and the brain stem (Supplementary Figure 1) consistent with published  
309 studies (Gregg et al., 2010b, 2010a; DeVeale et al., 2012). We therefore examined  
310 data from a single cell type to complement this analysis. Transcriptomic data analysis  
311 in neural stem cells from C57Bl/6J x JF1 hybrids (Bouschet et al., 2017) can be utilized

312 to assay allele-specificity by counting the number of aligned sequencing reads  
313 originating from each parental allele using SNPs between the two mouse strains. In  
314 neural stem cells there is low expression of *Ddc*, but a slight paternal bias of  
315 expression is detected at a number of different SNPs (albeit in the common part of  
316 the gene with *Ddc* canonical) (Supplementary Figure 1 C,D).

317  
318 Antisense transcripts are involved in imprinted gene regulation at several well  
319 characterized loci (Sleutels et al., 2002; Redrup et al., 2009). The *AK006690* transcript  
320 at this locus is annotated as transcribed in the antisense direction to *Ddc\_exon1a* and  
321 its expression was confirmed in newborn brain, heart and liver (data not shown).  
322 *AK006690* was assayed for allele-specific expression in heart and brain at E13.5,  
323 E16.5/E15.5 and newborn stages in mouse reciprocal hybrids. The transcript was  
324 found to be expressed from both parental alleles in brain and heart at E13.5 with a  
325 bias towards expression from the paternal allele in later stages of development in  
326 heart (Supplementary Fig 2). The observed allelic expression bias also can have a  
327 genetic cause, for example the influence of a nearby SNP on the amplification  
328 efficiency, but reciprocal hybrid assays suggest that the parental expression in heart  
329 at later stages is from the paternal allele (Supplementary Fig 2).

330

### 331 **Characterization of a *Ddc\_exon1a* deleted mouse model**

332 *Ddc\_exon1a* is expressed from the paternal allele in developing heart (Menheniott et  
333 al., 2008) therefore mice inheriting a null allele through the paternal line do not  
334 express *Ddc\_exon1a* in this tissue. Four genotypes were assayed for expression;  
335 *Ddc<sup>WT</sup>*, *Ddc<sup>MATΔ</sup>* (maternal deletion), *Ddc<sup>PATΔ</sup>* (paternal deletion) and *Ddc<sup>ΔΔ</sup>* (deletion

336 on both alleles). Quantitative PCR showed diminished expression in *Ddc<sup>PATΔ</sup>*  
337 compared to *Ddc<sup>WT</sup>* and *Ddc<sup>MATΔ</sup>* embryos (Supplementary Figure 3). There is a minor  
338 contribution from the maternal allele in the *Ddc<sup>PATΔ</sup>* genotype with the majority being  
339 derived from the paternal allele (Supplementary Figure 3), an observation that is  
340 consistent with imprinted gene expression (Horsthemke et al., 2011; Korostowski et  
341 al., 2011). DDC protein was not detected in *Ddc<sup>ΔΔ</sup>* animals (Supplementary Figure 3).

342  
343 Morphological changes at key sites of cardiac *Ddc* expression, including the width of  
344 the IVS and the thickness of the compact layer at the apical region of the right  
345 ventricle were measured in the *Ddc<sup>PATΔ</sup>* heart. An episcopic system (Rosenthal et al.,  
346 2004) was used to eliminate distortions associated with sectioning at e15.5 in hearts  
347 from *Ddc<sup>WT</sup>* (n=6), and *Ddc<sup>PATΔ</sup>* (n=3) animals which were all scored blind to the  
348 genotype. *Ddc<sup>PATΔ</sup>* embryos had a thinner compact layer in the right ventricle  
349 compared to *Ddc<sup>WT</sup>* by 0.019μm (Figure 3). A Mann-Whitney test did not reveal a  
350 difference in these measurements at a significance level of 5 % (p= 0.0952) with the  
351 number of mice examined but does suggest the possibility of thinning in the mutants.  
352 Thinning of the RV compact layer in the three ablated three ablated embryos could  
353 be the result of several different mechanisms (decreased myocyte proliferation,  
354 increased myocyte apoptosis, decreased progenitor cell expansion in the secondary  
355 heart field, or altered endocardial myocardial interactions) and further mechanistic  
356 resolution would be useful but is beyond the scope of this study. No statistically  
357 significant differences between *Ddc<sup>WT</sup>* and *Ddc<sup>PATΔ</sup>* were observed for the septum  
358 thickness or overall embryo size measured by crown-rump length again measured  
359 blind to genotype.

360

361 Expression microarrays were performed between *Ddc*<sup>WT</sup> and *Ddc*<sup>ΔΔ</sup> mice and the  
362 major difference detected was the *Ddc* gene itself (Supplementary Table 1). The  
363 modest impact on the transcriptome might be because the samples were  
364 heterogeneous or because the *Ddc*<sup>WT</sup> and *Ddc*<sup>MATΔ</sup> were combined as were the  
365 *Ddc*<sup>PATΔ</sup> and *Ddc*<sup>ΔΔ</sup>. Perturbations in molecular pathways could explain associated  
366 phenotypes and the ontology analysis (Supplementary Table 1) supports a role for  
367 DDC in cardiomyocyte growth and proliferation.

368

#### 369 **Imprinted expression of *DDC\_EXON1A* in human heart tissues**

370 The organisation of the *Ddc/Grb10* locus is conserved between mouse and human  
371 where it is located on Chromosome 7 in the human genome (Hitchins et al., 2002).  
372 Studies have shown that *DDC* is expressed from both parental alleles in several tissues  
373 from six human fetuses (Hitchins et al., 2002) but heart had not been assayed. We  
374 sequenced for SNPs in 25 human fetal hearts to test for monoallelic and parent-of-  
375 origin-specific expression of *DDC\_EXON1A*. A SNP was present in three informative  
376 samples, two displayed mono-allelic expression (Figure 4 A,B), the third showed a  
377 biased expression (Figure 4C). A further 15 fetal heart samples were collected with  
378 matched maternal genomic DNA and these were sequenced for SNPs. A SNP was  
379 found in two informative samples, sample 11886 showed biased expression from the  
380 paternal allele (Figure 4D) and 11908 showed paternal expression (Figure 4E).  
381 Polymorphic imprinting patterns are consistent with findings at other human  
382 imprinted loci such as *IGF2* (Giannoukakis et al., 1996) where inter-individual

383 variation in parental allele-specific expression/imprinting has been documented as  
384 well as more broadly at other imprinted loci across the genome (Zink et al., 2018).

385

## 386 **Discussion**

### 387 ***Ddc\_exon1A* imprinted expression**

388 *Ddc\_exon1a* is paternally expressed in the developing mouse heart. Immunostaining  
389 of sectioned mouse hearts reveals strong signal in the region of the secondary heart  
390 field where progenitor cells go on to form the distal parts of the outflow tract and  
391 arterial trunks, right ventricle and interventricular system. Abnormal development in  
392 any of these components of cardiac development can result in congenital heart  
393 disease (Chaudhry et al., 2014; Kelly et al., 2014) and the importance of right  
394 ventricular abnormalities in the pathology of cardiovascular disease in the adult has  
395 recently been an intense area of investigation (Amsallem et al., 2018).

396

397 As is typical for imprinted genes, *Ddc\_exon1a* exists in an imprinting cluster, sharing  
398 an imprinting control region (ICR) with the *Grb10* gene. The deletion of the ICR on the  
399 paternal allele in mouse heart results in the silencing of the active paternal  
400 *Ddc\_exon1a* allele indicating that imprinted *Ddc\_exon1a* expression in heart is  
401 governed by the ICR via a *cis*-acting mechanism. Deletion of the maternally inherited  
402 ICR does not alter expression of *Ddc\_exon1a* in heart (Shiura et al., 2009) because the  
403 maternal allele is normally epigenetically silenced. Investigating the tissue  
404 distribution of *Ddc\_exon1a* and *Grb10* is an important step for examining the  
405 regulatory relationship between these two clustered genes. Given that *Ddc\_exon1a*  
406 is highly tissue-specific in its expression, the spatial distribution of these genes was

407 examined in the developing heart and appeared to be non-overlapping. Paternal  
408 *Grb10* gene expression and DDC protein localisation (Figure 2) suggests that paternal  
409 *Ddc\_exon1a* and paternal *Grb10* imprinted gene expression is not coupled in the  
410 heart.

411  
412 *Grb10* is also oppositely imprinted (paternally expressed) in the brain compared to  
413 most other tissues and this suggested that brain could also be a useful tissue in which  
414 to examine the imprinted expression of *Ddc\_exon1a* for the identification of tissue-  
415 specific imprinting mechanisms. However, *Ddc\_exon1a* is not imprinted in the brain  
416 of neonatal mice (Supplementary Figure 2) implying that the epigenetic control of  
417 *Ddc\_exon1a* imprinting is unlikely to be co-ordinated with *Grb10* in brain, although  
418 paternal expression was reported in NSCs. The ICR seems only to influence tissue-  
419 specific imprinting of *Ddc\_exon1a* in the heart. It is possible that at the individual cell  
420 type level, *Ddc\_exon1a* could be imprinted in brain because *Grb10* exhibits imprinting  
421 in neurons, but the signal is masked by the maternal expression of *Grb10* in glia  
422 (Yamasaki-Ishizaki et al., 2007) and so there could be some cell-specific expression  
423 co-ordination (Tucci et al., 2019).

424  
425 Antisense transcripts are involved in imprinted gene regulation at several well  
426 characterized loci (Sleutels et al., 2002). If the *AK006690* transcript was involved in  
427 the mechanism of imprinting at *Ddc\_exon1a*, it would be predicted to be maternally  
428 expressed in heart based on imprinting mechanisms at other loci. However, we  
429 detected biallelic (at E15.5) or paternally biased expression (E16.5 and nb) which  
430 discounts an obvious mechanistic role for *AK006690* in the imprinting of *Ddc\_exon1a*.

431

432 **DDC function in heart**

433 Homozygous null mice for *Ddc* die late in prenatal development (Eppig et al., 2012),  
434 likely due to a lack of neurotransmitter synthesis in the brain and CNS. However, mice  
435 harbouring a deletion of the *Ddc\_exon1a* allele inherited through the paternal line  
436 only (*Ddc<sup>PatΔ</sup>*), are knockouts for *Ddc* in heart due to its imprinted status and the  
437 expression pattern of the *Ddc\_Exon1A* isoform. [In the small number of animals](#)  
438 [studied](#), compared to the wildtype littermates, *Ddc<sup>PATΔ</sup>* mice [tend to](#) have right  
439 ventricular hypoplasia of the myocardium at the region that exhibits the most  
440 abundant *Ddc* expression at e15.5 (Figure 3 & Supplementary Fig 3) pointing to a role  
441 for DDC in myocardial growth. *Ddc* is expressed mainly in the myocardium of the right  
442 ventricle and IVS. These structures are derived from the secondary heart field (SHF)  
443 population of myocardial progenitors (Kelly, 2012) further delineating the SHF as a  
444 unique myocardial population distinct from the first heart field (FHF) and suggesting  
445 that *Ddc* plays a role in SHF ontogeny.

446

447 Gene expression differences between *Ddc<sup>PATΔ</sup>* and *Ddc<sup>WT</sup>* hearts were found at *Ddc*  
448 itself, with only modest differences of other genes (Supplementary Table 1). DDC may  
449 not therefore function to directly mediate gene expression in the heart, but instead  
450 results in biochemical changes that influence local gene expression via feedback  
451 mechanisms. Of note, *Ddc* expression is not ubiquitous throughout the heart and is  
452 not expressed in all ventricular myocytes. There is also no detectable expression in  
453 other cardiac cell populations such as the endocardium or epicardium. This  
454 heterogeneity of expression, with expression limited to the septum and apical



455 portion of the RV may mask changes in gene expression in *Ddc*<sup>PATΔ</sup> cells when pooled  
456 in bulk cell analyses such as microarrays with cell populations not affected by  
457 alterations in *Ddc* expression. Further evaluation of the impact of DDC deletion will  
458 require single cell transcriptomic analysis.

459

#### 460 **Human *DDC\_EXON1A* imprinting**

461 *DDC\_EXON1A* displays polymorphic monoallelic expression in the developing human  
462 heart, and where there is monoallelic expression, this is from the paternal allele as  
463 observed in the mouse. The NHGRI-EBI Catalog of published genome-wide  
464 association studies does not currently report mutations in DDC that relate to heart  
465 development or cardiomyopathy. However, hypermethylation of the GRB10 ICR in  
466 peripheral blood samples has recently been associated with congenital heart disease  
467 (Chang et al., 2021). The complex pattern of tissue-specific imprinted expression at  
468 this locus suggests it may warrant special consideration in genetic studies because  
469 *Ddc\_exon1a* ablation has a mild effect on the developing heart and with a small effect  
470 size there could be moderately widespread ablation of this exon in human  
471 populations that presents a suitable genetic background for other mutations to cause  
472 developmental abnormalities.

473

474 In summary, *Ddc\_exon1a* is a heart-specific imprinted isoform expressed from the  
475 paternally inherited allele regulated by differential DNA methylation at an ICR in the  
476 adjacent *Grb10* gene but not by the expression of *Grb10* itself. When ablated via gene  
477 knock-out in the heart, morphological changes are detected in small numbers of  
478 embryos. While IVS thickness was observed but it is important to note that RV

479 function was not assessed and it is reasonable to suspect that abnormal RV function  
480 might contribute to the late embryonic lethality observed in *Ddc* mutants. In humans,  
481 *DDC\_EXON1A* gene expression has a paternal bias and is polymorphically imprinted,  
482 a finding common among imprinted genes in humans (Monk et al., 2006).

483

#### 484 **Conflict of Interest**

485 The authors declare that the research was conducted in the absence of any  
486 commercial or financial relationships that could be construed as a potential conflict  
487 of interest.

#### 488 **Author contributions**

489 AP conducted experiments, interpreted data and contributed to writing the paper,  
490 SMA, MF, MC, WP, MS, BM conducted experiments; MDI collected human tissue  
491 samples; BM, NB, RS designed and performed data analyses; MM-S and AW provided  
492 and collected Grb10 transgenic tissue samples; HSB conceived the EFIC analysis and  
493 provided EFIC facilities, supervised AP and interpreted the heart sections and EFIC  
494 data; RJO conceived the project, supervised the project, interpreted the data and  
495 wrote the paper with AP. All authors contributed to the critical reading and editing of  
496 the manuscript.

497

#### 498 **Funding**

499 This work was supported by the British Heart Foundation Project Grant  
500 [PG/13/35/30236] (RJO) and PhD studentship FS/08/051/25748 (to RJO undertaken  
501 by ARP); the Wellcome Trust Project Grant [084358/Z/07/Z] (RJO); the Medical  
502 Research Council Project Grant [G1001689] (RJO); the National Institutes of Health

503 [1R01 HL118386] (HSB); and EFIC facility, the National Institute of Health [S10-  
504 RR27661] (HSB).

505

## 506 **Acknowledgements**

507 We thank Dr Matt Arno and the KCL genomics facility for core equipment usage. The  
508 authors acknowledge support from the Department of Health via the National  
509 Institute for Health Research (NIHR) Biomedical Research Centre at Guy's and St  
510 Thomas' NHS Foundation Trust in partnership with King's College London for access  
511 to the genomics core facility at the time directed by Dr Alka Saxena. We thank James  
512 Cain for help with the Figures, Dr Heba Saadeh for assistance with bioinformatics  
513 analysis of the expression microarray and Dr Sabrina Böhm for technical support. We  
514 thank the MRC-Wellcome Trust Human Developmental Biology Resource (HDBR)  
515 (<http://www.hdbr.org>) from the Institute of Genetic Medicine, Newcastle and  
516 Institute of Child Health, London for human fetal tissues.

517

## 518 **References**

519 Amsallem, M., Mercier, O., Kobayashi, Y., Moneghetti, K., and Haddad, F.

520 (2018). Forgotten No More: A Focused Update on the Right Ventricle  
521 in Cardiovascular Disease. *JACC Hear. Fail.* 6, 891–903.

522 doi:10.1016/j.jchf.2018.05.022.

523 Barlow, D. P., and Bartolomei, M. S. (2014). Genomic imprinting in  
524 mammals. *Cold Spring Harb Perspect Biol* 6.

525 doi:10.1101/cshperspect.a018382.

526 Bouschet, T., Dubois, E., Reynès, C., Kota, S. K., Rialle, S., Maupetit-

527 Méhouas, S., et al. (2017). In Vitro Corticogenesis from Embryonic  
528 Stem Cells Recapitulates the In Vivo Epigenetic Control of Imprinted  
529 Gene Expression. *Cereb. cortex* 27, 2418–2433.  
530 doi:10.1093/cercor/bhw102.

531 Chang, S., Wang, Y., Xin, Y., Wang, S., Luo, Y., Wang, L., et al. (2021). DNA  
532 methylation abnormalities of imprinted genes in congenital heart  
533 disease: a pilot study. *BMC Med. Genomics* 14, 1–11.  
534 doi:10.1186/s12920-020-00848-0.

535 Charalambous, M., Smith, F. M., Bennett, W. R., Crew, T. E., Mackenzie, F.,  
536 and Ward, A. (2003). Disruption of the imprinted Grb10 gene leads to  
537 disproportionate overgrowth by an Igf2-independent mechanism.  
538 *Proc. Natl. Acad. Sci. U. S. A.* 100, 8292–8297.  
539 doi:10.1073/pnas.1532175100.

540 Chaudhry, B., Ramsbottom, S., and Henderson, D. J. (2014). “Chapter Two -  
541 Genetics of Cardiovascular Development,” in *Genetics of*  
542 *Cardiovascular Disease*, ed. T. J. A. B. T.-P. in M. B. and T. S. Chico  
543 (Academic Press), 19–41. doi:[https://doi.org/10.1016/B978-0-12-](https://doi.org/10.1016/B978-0-12-386930-2.00002-1)  
544 [386930-2.00002-1](https://doi.org/10.1016/B978-0-12-386930-2.00002-1).

545 Cleaton, M. A. M., Edwards, C. A., and Ferguson-Smith, A. C. (2014).  
546 Phenotypic Outcomes of Imprinted Gene Models in Mice: Elucidation  
547 of Pre- and Postnatal Functions of Imprinted Genes. *Annu. Rev.*  
548 *Genomics Hum. Genet.* 15, 93–126. doi:10.1146/annurev-genom-  
549 091212-153441.

550 DeVeale, B., van der Kooy, D., and Babak, T. (2012). Critical evaluation of

551 imprinted gene expression by RNA-Seq: a new perspective. *PLoS*  
552 *Genet* 8, e1002600. doi:10.1371/journal.pgen.1002600.

553 Edwards, C. A., and Ferguson-Smith, A. C. (2007). Mechanisms regulating  
554 imprinted genes in clusters. *Curr. Opin. Cell Biol.* 19, 281–289.  
555 doi:10.1016/j.ceb.2007.04.013.

556 Eppig, J. T., Blake, J. A., Bult, C. J., Kadin, J. A., and Richardson, J. E. (2012).  
557 The Mouse Genome Database (MGD): comprehensive resource for  
558 genetics and genomics of the laboratory mouse. *Nucleic Acids Res* 40,  
559 D881-6. doi:gkr974 [pii]10.1093/nar/gkr974.

560 Ferrón, S. R., Charalambous, M., Radford, E., McEwen, K., Wildner, H.,  
561 Hind, E., et al. (2011). Postnatal loss of Dlk1 imprinting in stem cells  
562 and niche astrocytes regulates neurogenesis. *Nature* 475, 381–385.  
563 doi:10.1038/nature10229.

564 Garfield, A. S., Cowley, M., Smith, F. M., Moorwood, K., Stewart-Cox, J. E.,  
565 Gilroy, K., et al. (2011). Distinct physiological and behavioural  
566 functions for parental alleles of imprinted Grb10. *Nature* 469, 534–  
567 538. doi:10.1038/nature09651.

568 Giannoukakis, N., Deal, C., Paquette, J., Kukuvtis, A., and Polychronakos, C.  
569 (1996). Polymorphic functional imprinting of the human IGF2 gene  
570 among individuals, in blood cells, is associated with H19 expression.  
571 *Biochem Biophys Res Commun* 220, 1014–1019.  
572 doi:10.1006/bbrc.1996.0524.

573 Gregg, C., Zhang, J., Butler, J. E., Haig, D., and Dulac, C. (2010a). Sex-specific  
574 parent-of-origin allelic expression in the mouse brain. *Science* (80-. ).

575 329, 682–685. doi:10.1126/science.1190831.

576 Gregg, C., Zhang, J., Weissbourd, B., Luo, S., Schroth, G. P., Haig, D., et al.

577 (2010b). High-resolution analysis of parent-of-origin allelic expression

578 in the mouse brain. *Science* (80-. ). 329, 643–648. doi:science.1190830

579 [pii]10.1126/science.1190830.

580 Hitchins, M. P., Bentley, L., Monk, D., Beechey, C., Peters, J., Kelsey, G., et

581 al. (2002). DDC and COBL, flanking the imprinted GRB10 gene on

582 7p12, are biallelically expressed. *Mamm Genome* 13, 686–691.

583 doi:10.1007/s00335-002-3028-z.

584 Horsthemke, B., Wawrzik, M., Groß, S., Lich, C., Sauer, B., Rost, I., et al.

585 (2011). Parental origin and functional relevance of a de novo UBE3A

586 variant. *Eur. J. Med. Genet.* 54, 19–24.

587 doi:10.1016/j.ejmg.2010.09.005.

588 Ideraabdullah, F. Y., Vigneau, S., and Bartolomei, M. S. (2008). Genomic

589 imprinting mechanisms in mammals. *Mutat. Res.* 647, 77–85.

590 doi:10.1016/j.mrfmmm.2008.08.008.

591 Kelly, R. G. (2012). The second heart field. *Curr Top Dev Biol* 100, 33–65.

592 doi:10.1016/B978-0-12-387786-4.00002-6.

593 Kelly, R. G., Buckingham, M. E., and Moorman, A. F. (2014). Heart fields and

594 cardiac morphogenesis. *Cold Spring Harb. Perspect. Med.* 4, 1–11.

595 doi:10.1101/cshperspect.a015750.

596 Kelsey, G., and Bartolomei, M. S. (2012). Imprinted Genes ... and the

597 Number Is? *PLoS Genet.* 8, e1002601.

598 doi:10.1371/journal.pgen.1002601.g001.

599 Korostowski, L., Raval, A., Breuer, G., and Engel, N. (2011). Enhancer-driven  
600 chromatin interactions during development promote escape from  
601 silencing by a long non-coding RNA. *Epigenetics Chromatin* 4, 21.  
602 doi:10.1186/1756-8935-4-21.

603 Lajiness, J. D., and Conway, S. J. (2014). Origin, development, and  
604 differentiation of cardiac fibroblasts. *J. Mol. Cell. Cardiol.* 70, 2–8.  
605 doi:10.1016/j.yjmcc.2013.11.003.

606 Lee, N. C., Shieh, Y. D., Chien, Y. H., Tzen, K. Y., Yu, I. S., Chen, P. W., et al.  
607 (2013). Regulation of the dopaminergic system in a murine model of  
608 aromatic L-amino acid decarboxylase deficiency. *Neurobiol Dis* 52,  
609 177–190. doi:10.1016/j.nbd.2012.12.005.

610 Lewis, A., and Reik, W. (2006). How imprinting centres work. *Cytogenet.*  
611 *Genome Res.* 113, 81–89. doi:10.1159/000090818.

612 Madon-Simon, M., Cowley, M., Garfield, A. S., Moorwood, K., Bauer, S. R.,  
613 and Ward, A. (2014). Antagonistic roles in fetal development and adult  
614 physiology for the oppositely imprinted Grb10 and Dlk1 genes. *BMC*  
615 *Biol.* 12, 771. doi:10.1186/s12915-014-0099-8.

616 Menheniott, T. R., Woodfine, K., Schulz, R., Wood, A. J., Monk, D., Giraud,  
617 A. S., et al. (2008). Genomic imprinting of Dopa decarboxylase in heart  
618 and reciprocal allelic expression with neighboring Grb10. *Mol. Cell.*  
619 *Biol.* 28, 386–396. doi:10.1128/MCB.00862-07.

620 Monk, D., Arnaud, P., Apostolidou, S., Hills, F. A., Kelsey, G., Stanier, P., et  
621 al. (2006). Limited evolutionary conservation of imprinting in the  
622 human placenta. *Proc. Natl. Acad. Sci.* 103, 6623–6628.

623 doi:10.1073/pnas.0511031103.

624 Plasschaert, R. N., and Bartolomei, M. S. (2015). Tissue-specific regulation  
625 and function of Grb10 during growth and neuronal commitment. *Proc.*  
626 *Natl. Acad. Sci. U. S. A.* 112, 6841–6847.  
627 doi:10.1073/pnas.1411254111.

628 Redrup, L., Branco, M. R., Perdeaux, E. R., Krueger, C., Lewis, A., Santos, F.,  
629 et al. (2009). The long noncoding RNA Kcnq 1ot1 organises a lineage-  
630 specific nuclear domain for epigenetic gene silencing. *Development*  
631 136, 525–530. doi:10.1242/dev.031328.

632 Rosenthal, J., Mangal, V., Walker, D., Bennett, M., Mohun, T. J., and Lo, C.  
633 W. (2004). Rapid high resolution three dimensional reconstruction of  
634 embryos with episcopic fluorescence image capture. *Birth Defects Res.*  
635 *Part C Embryo Today Rev.* 72, 213–223. doi:10.1002/bdrc.20023.

636 Shiura, H., Nakamura, K., Hikichi, T., Hino, T., Oda, K., Suzuki-Migishima, R.,  
637 et al. (2009). Paternal deletion of Meg1/Grb10 DMR causes  
638 maternalization of the Meg1/Grb10 cluster in mouse proximal  
639 Chromosome 11 leading to severe pre- and postnatal growth  
640 retardation. *Hum. Mol. Genet.* 18, 1424–1438.  
641 doi:10.1093/hmg/ddp049.

642 Sleutels, F., Zwart, R., and Barlow, D. P. (2002). The non-coding Air RNA is  
643 required for silencing autosomal imprinted genes. *Nature* 415, 810–  
644 813. doi:10.1038/415810a.

645 Smith, C. M., Finger, J. H., Hayamizu, T. F., McCright, I. J., Xu, J., Berghout,  
646 J., et al. (2014). The mouse Gene Expression Database (GXD): 2014



647 update. *Nucleic Acids Res* 42, D818-24. doi:10.1093/nar/gkt954.

648 Smith, F. M., Holt, L. J., Garfield, A. S., Charalambous, M., Koumanov, F.,  
649 Perry, M., et al. (2007). Mice with a Disruption of the Imprinted Grb10  
650 Gene Exhibit Altered Body Composition, Glucose Homeostasis, and  
651 Insulin Signaling during Postnatal Life. *Mol. Cell. Biol.* 27, 5871–5886.  
652 doi:10.1128/MCB.02087-06.

653 Smyth, G. K. (2004). Linear models and empirical bayes methods for  
654 assessing differential expression in microarray experiments. *Stat Appl*  
655 *Genet Mol Biol* 3, Article3. doi:10.2202/1544-6115.1027.

656 Tucci, V., Isles, A. R., Kelsey, G., Ferguson-Smith, A. C., Bartolomei, M. S.,  
657 Benvenisty, N., et al. (2019). Genomic Imprinting and Physiological  
658 Processes in Mammals. *Cell* 176, 952–965.  
659 doi:10.1016/j.cell.2019.01.043.

660 Yamasaki-Ishizaki, Y., Kayashima, T., Mapendano, C. K., Soejima, H., Ohta,  
661 T., Masuzaki, H., et al. (2007). Role of DNA methylation and histone H3  
662 lysine 27 methylation in tissue-specific imprinting of mouse Grb10.  
663 *Mol. Cell. Biol.* 27, 732–742. doi:10.1128/MCB.01329-06.

664 Zink, F., Magnusdottir, D. N., Magnusson, O. T., Walker, N. J., Morris, T. J.,  
665 Sigurdsson, A., et al. (2018). Insights into imprinting from parent-of-  
666 origin phased methylomes and transcriptomes. *Nat. Genet.* 50.  
667 doi:10.1038/s41588-018-0232-7.

668

## 669 **Figure Legends**

670 **Figure 1**

671 DDC in e15.5 and e18.5 hearts. Coronal sections of the heart co-stained for DDC (red)  
672 and the myocardial marker MF-20 (green) (A,B,C) and DDC and a marker of trabeculae,  
673 ANF (green) (D-I). DDC protein (red) is present throughout the ventricular  
674 myocardium and interventricular septum (IVS), the structure separating the right and  
675 left ventricles, (B, E H), but absent from the atria and the trabecular layer, except  
676 where the trabeculae meet the compact myocardial layer (D-I). This is also seen in  
677 sagittal sections at e18.5 (J, K, L) where DDC is present in the myocardium, IVS, and  
678 right ventricular myocardium. Blue staining is DAPI nuclear counterstain (A,D,G,J,K,L).  
679 RV Right Ventricle, LV Left Ventricle, RA Right Atrium, LA Left Atrium. Minimum  
680 number of hearts examined =3.

681 **Figure 2**

682 Analysis of paternal *Grb10* expression and DDC protein staining in e18.5 heart serial  
683 sections. (A) & (B) are serial sections in the sagittal plane showing the right ventricle  
684 (RV) and the left ventricle (LV). (C) and (D) are serial sections showing only the RV  
685 where DDC staining is most abundant. (A) and (C) are stained with X-gal to reveal  
686 paternal *Grb10* expression in blue from the lacZ reporter construct and the  
687 counterstaining is pink. (B) and (D) are stained for DDC protein using DAB (brown) via  
688 immunohistochemistry, counterstaining is pale green. DDC protein distribution is  
689 extensive compared to *Grb10* which is restricted to the inter ventricular septum (IVS).  
690 Minimum number of hearts examined =3, maximum number =6.

691 **Figure 3**

692 Morphological analysis of *Ddc* knockout hearts. Episcopic fluorescence image capture  
693 measurements of wildtype *Ddc*<sup>WT</sup> and *Ddc*<sup>PATΔ</sup> knockout e15.5 mouse heart regions  
694 using embedded, sequentially sectioned hearts built into a 3D model using the

695 Velocity™ software. Visualisation of the 3D ventricles depicting where the  
696 measurements were made in (A) *Ddc*<sup>WT</sup> and (B) *Ddc*<sup>PATΔ</sup> embryos. The thickness of the  
697 right ventricle (RV) compact myocardium at the apical point parallel to the  
698 interventricular septum (IVS) is shown by the pink bar in (A) and pink bar in (B). The  
699 IVS measured at the widest point is indicated by the turquoise bar in (A) and the  
700 turquoise bar in (B). All measurements were adjusted to crown rump length to  
701 control for embryo size variation (C) (D) (E). There was a [trend towards a decrease](#) in  
702 thickness of the compact layer in the right ventricle (C) in knockout animal hearts  
703 compared to wild type with no change in the width of the IVS (D) or crown-rump  
704 length (E) [but the total numbers of embryos studied was not sufficient to show](#)  
705 [statistical significance](#).

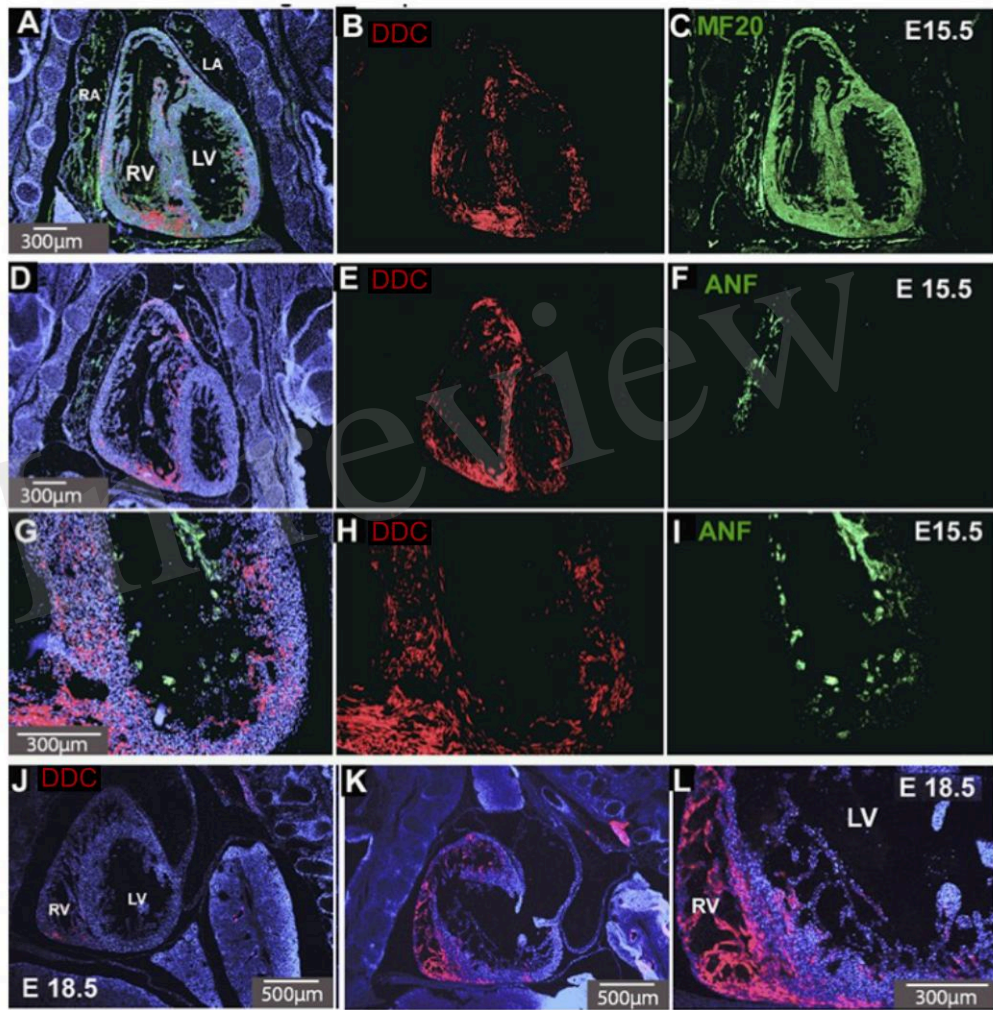
706 **Figure 4**

707 A, B, human fetal heart allele-specific assays, informative samples from 25 hearts  
708 collected from a tissue bank. Individuals in panel A and B are mono allelic (one peak  
709 across the SNP) and the individual in panel C presented with a biallelic pattern of  
710 expression (2 peaks across the SNP). SNPs annotated in the UCSC genome browser  
711 were identified in these individuals by sequencing genomic (g)DNA in the forward (F)  
712 and reverse (R) directions but allelic origin could not be assigned without parental  
713 samples. The SNP is indicated by a vertical line. Panels D, E, human fetal heart allele-  
714 specific assays, informative samples from 15 individual hearts with both fetal and  
715 maternal DNA samples. SNPs annotate in the UCSC genome browser were identified  
716 by sequencing with flanking primers in gDNA from the mother (single peak) and fetus  
717 (double peak) in the upper panels. Allele-specific assays amplifying and sequencing  
718 cDNA from fetal heart RNA are in the lower panels. Sample 11886 has both peaks

719 indicating expression from the maternal and paternal alleles whereas mono-allelic  
720 paternal expression of DDC\_EXON1A is detected in 11908.

In review

Figure 1.JPEG



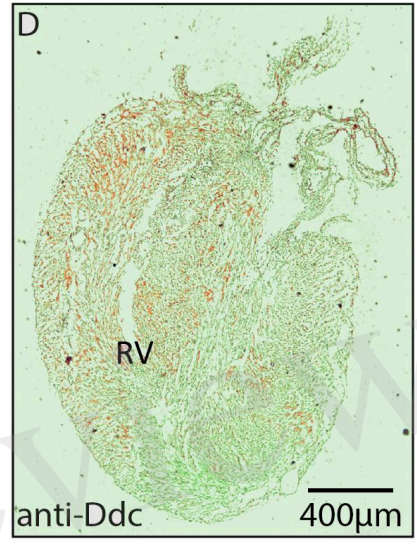
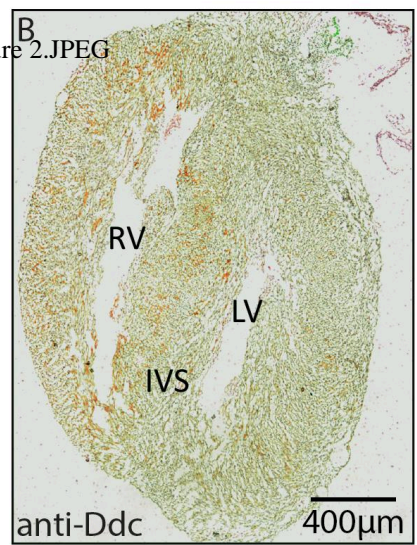
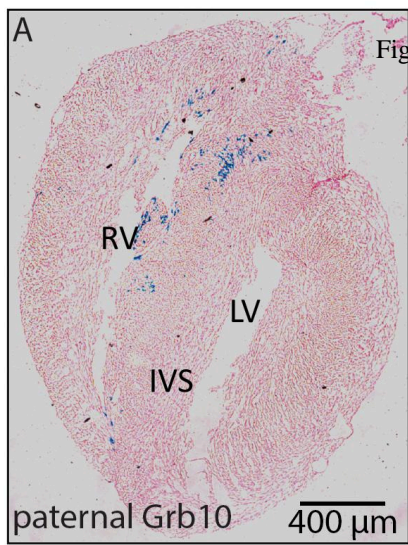
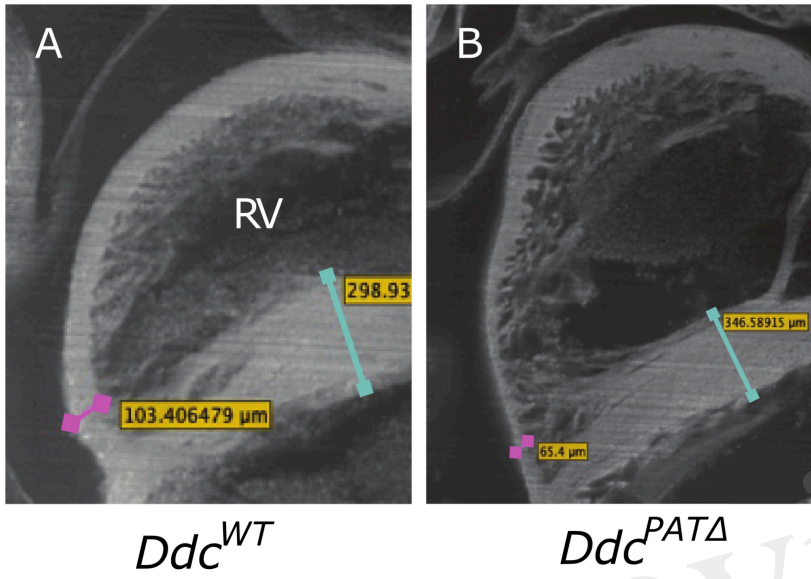
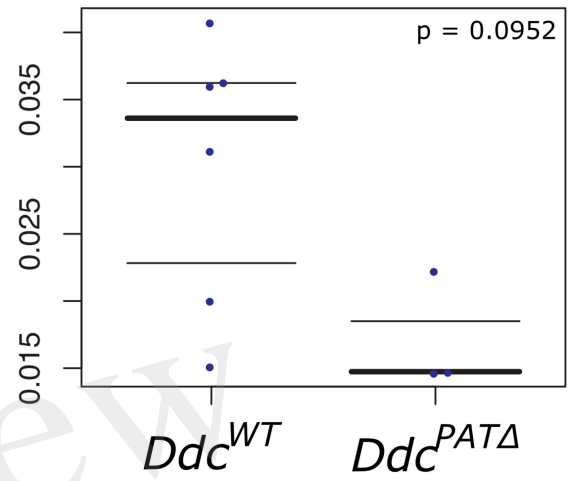


Figure 2.JPEG

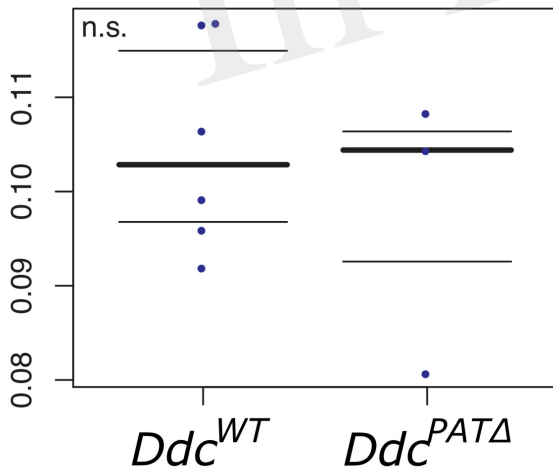
Figure 3.JPEG



### C Right ventricle compact myocardium



### D Interventricular Septum



### E Crown-rump length

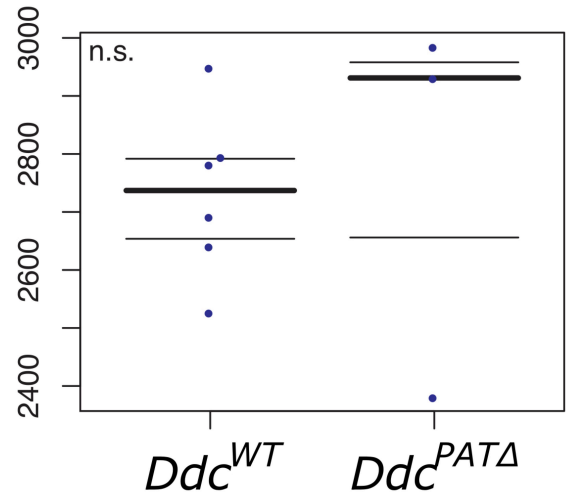


Figure 4.JPEG

